

Search for Trilepton Nucleon Decay via $p \rightarrow e^+ \nu \nu$ and $p \rightarrow \mu^+ \nu \nu$ in the Super-Kamiokande Experiment

V. Takhistov,⁷ K. Abe,^{1,29} Y. Haga,¹ Y. Hayato,^{1,29} M. Ikeda,¹ K. Iyogi,¹ J. Kameda,^{1,29} Y. Kishimoto,^{1,29} M. Miura,^{1,29} S. Moriyama,^{1,29} M. Nakahata,^{1,29} Y. Nakano,¹ S. Nakayama,^{1,29} H. Sekiya,^{1,29} M. Shiozawa,^{1,29} Y. Suzuki,^{1,29} A. Takeda,^{1,29} H. Tanaka,¹ T. Tomura,^{1,29} K. Ueno,¹ R. A. Wendell,^{1,29} T. Yokozawa,¹ T. Irvine,² T. Kajita,^{2,29} I. Kametani,² K. Kaneyuki,^{2,29,*} K. P. Lee,² T. McLachlan,² Y. Nishimura,² E. Richard,² K. Okumura,^{2,29} L. Labarga,³ P. Fernandez,³ S. Berkman,⁵ H. A. Tanaka,⁵ S. Tobayama,⁵ J. Gustafson,⁴ E. Kearns,^{4,29} J. L. Raaf,⁴ J. L. Stone,^{4,29} L. R. Sulak,⁴ M. Goldhaber,^{6,*} G. Carminati,⁷ W. R. Kropp,⁷ S. Mine,⁷ P. Weatherly,⁷ A. Renshaw,⁷ M. B. Smy,^{7,29} H. W. Sobel,^{7,29} K. S. Ganezer,⁸ B. L. Hartfiel,⁸ J. Hill,⁸ W. E. Keig,⁸ N. Hong,⁹ J. Y. Kim,⁹ I. T. Lim,⁹ T. Akiri,¹⁰ A. Himmel,¹⁰ K. Scholberg,^{10,29} C. W. Walter,^{10,29} T. Wongjirad,¹⁰ T. Ishizuka,¹¹ S. Tasaka,¹² J. S. Jang,¹³ J. G. Learned,¹⁴ S. Matsuno,¹⁴ S. N. Smith,¹⁴ T. Hasegawa,¹⁵ T. Ishida,¹⁵ T. Ishii,¹⁵ T. Kobayashi,¹⁵ T. Nakadaira,¹⁵ K. Nakamura,^{15,29} Y. Oyama,¹⁵ K. Sakashita,¹⁵ T. Sekiguchi,¹⁵ T. Tsukamoto,¹⁵ A. T. Suzuki,¹⁶ Y. Takeuchi,¹⁶ C. Bronner,¹⁷ S. Hirota,¹⁷ K. Huang,¹⁷ K. Ieki,¹⁷ T. Kikawa,¹⁷ A. Minamino,¹⁷ A. Murakami,¹⁷ T. Nakaya,^{17,29} K. Suzuki,¹⁷ S. Takahashi,¹⁷ K. Tateishi,¹⁷ Y. Fukuda,¹⁸ K. Choi,¹⁹ Y. Itow,¹⁹ G. Mitsuka,¹⁹ P. Mijakowski,³⁴ J. Hignight,²⁰ J. Imber,²⁰ C. K. Jung,²⁰ C. Yanagisawa,²⁰ H. Ishino,²¹ A. Kibayashi,²¹ Y. Koshio,²¹ T. Mori,²¹ M. Sakuda,²¹ R. Yamaguchi,²¹ T. Yano,²¹ Y. Kuno,²² R. Tacik,^{23,31} S. B. Kim,²⁴ H. Okazawa,²⁵ Y. Choi,²⁶ K. Nishijima,²⁷ M. Koshihara,²⁸ Y. Suda,²⁸ Y. Totsuka,^{28,*} M. Yokoyama,^{28,29} K. Martens,²⁹ Ll. Marti,²⁹ M. R. Vagins,^{29,7} J. F. Martin,³⁰ P. de Perio,³⁰ A. Konaka,³¹ M. J. Wilking,³¹ S. Chen,³² Y. Zhang,³² K. Connolly,³³ and R. J. Wilkes³³

(The Super-Kamiokande Collaboration)

¹Kamioka Observatory, Institute for Cosmic Ray Research, University of Tokyo, Kamioka, Gifu 506-1205, Japan

²Research Center for Cosmic Neutrinos, Institute for Cosmic Ray Research, University of Tokyo, Kashiwa, Chiba 277-8582, Japan

³Department of Theoretical Physics, University Autonoma Madrid, 28049 Madrid, Spain

⁴Department of Physics, Boston University, Boston, MA 02215, USA

⁵Department of Physics and Astronomy, University of British Columbia, Vancouver, BC, V6T1Z4, Canada

⁶Physics Department, Brookhaven National Laboratory, Upton, NY 11973, USA

⁷Department of Physics and Astronomy, University of California, Irvine, Irvine, CA 92697-4575, USA

⁸Department of Physics, California State University, Dominguez Hills, Carson, CA 90747, USA

⁹Department of Physics, Chonnam National University, Kwangju 500-757, Korea

¹⁰Department of Physics, Duke University, Durham NC 27708, USA

¹¹Junior College, Fukuoka Institute of Technology, Fukuoka, Fukuoka 811-0295, Japan

¹²Department of Physics, Gifu University, Gifu, Gifu 501-1193, Japan

¹³GIST College, Gwangju Institute of Science and Technology, Gwangju 500-712, Korea

¹⁴Department of Physics and Astronomy, University of Hawaii, Honolulu, HI 96822, USA

¹⁵High Energy Accelerator Research Organization (KEK), Tsukuba, Ibaraki 305-0801, Japan

¹⁶Department of Physics, Kobe University, Kobe, Hyogo 657-8501, Japan

¹⁷Department of Physics, Kyoto University, Kyoto, Kyoto 606-8502, Japan

¹⁸Department of Physics, Miyagi University of Education, Sendai, Miyagi 980-0845, Japan

¹⁹Solar Terrestrial Environment Laboratory, Nagoya University, Nagoya, Aichi 464-8602, Japan

²⁰Department of Physics and Astronomy, State University of New York at Stony Brook, NY 11794-3800, USA

²¹Department of Physics, Okayama University, Okayama, Okayama 700-8530, Japan

²²Department of Physics, Osaka University, Toyonaka, Osaka 560-0043, Japan

²³Department of Physics, University of Regina, 3737 Wascana Parkway, Regina, SK, S4S0A2, Canada

²⁴Department of Physics, Seoul National University, Seoul 151-742, Korea

²⁵Department of Informatics in Social Welfare, Shizuoka University of Welfare, Yaizu, Shizuoka, 425-8611, Japan

²⁶Department of Physics, Sungkyunkwan University, Suwon 440-746, Korea

²⁷Department of Physics, Tokai University, Hiratsuka, Kanagawa 259-1292, Japan

²⁸The University of Tokyo, Bunkyo, Tokyo 113-0033, Japan

²⁹Kavli Institute for the Physics and Mathematics of the Universe (WPI), Todai Institutes for Advanced Study, University of Tokyo, Kashiwa, Chiba 277-8582, Japan

³⁰Department of Physics, University of Toronto, 60 St., Toronto, Ontario, M5S1A7, Canada

³¹TRIUMF, 4004 Wesbrook Mall, Vancouver, BC, V6T2A3, Canada

³²Department of Engineering Physics, Tsinghua University, Beijing, 100084, China

³³Department of Physics, University of Washington, Seattle, WA 98195-1560, USA

³⁴National Centre For Nuclear Research, 00-681 Warsaw, Poland

(Dated: September 9, 2014)

The trilepton nucleon decay modes $p \rightarrow e^+ \nu \nu$ and $p \rightarrow \mu^+ \nu \nu$ violate $|\Delta(B - L)|$ by two units. Using data from a 273.4 kiloton year exposure of Super-Kamiokande a search for these decays yields a fit consistent with no signal. Accordingly, lower limits on the partial lifetimes of $\tau_{p \rightarrow e^+ \nu \nu} > 1.7 \times 10^{32}$ years and $\tau_{p \rightarrow \mu^+ \nu \nu} > 2.2 \times 10^{32}$ years at a 90% confidence level are obtained. These limits can constrain Grand Unified Theories which allow for such processes.

PACS numbers: 12.10.Dm, 13.30.-a, 11.30.Fs, 12.60.Jv, 14.20.Dh, 29.40.Ka

There is strong theoretical motivation for a Grand Unified Theory (GUT) [1, 2] as an underlying description of nature. Unification of the running couplings, charge quantization, as well as other hints point to the Standard Model (SM) being an incomplete theory. Though the GUT energy scale is inaccessible to accelerator experiments a signature prediction of these theories is an unstable proton with lifetimes that can be probed by large underground experiments. Observation of proton decay would constitute strong evidence for physics beyond the SM, and non-observation imposes stringent constraints on GUT models.

One of the simplest unification scenarios, based on minimal SU(5), has been decisively ruled out by limits on $p \rightarrow e^+ \pi^0$ [3–5]. On the other hand, models based on minimal supersymmetric (SUSY) extensions are strongly constrained by bounds from $p \rightarrow \bar{\nu} K^+$ [6], and with signs of SUSY unobserved at the Large Hadron Collider (LHC) [7, 8], there is reinvigorated interest in other approaches and possible signatures. A popular scenario may be found in a left-right symmetric partial unification of Pati and Salam (PS) [9] and its embedding into SO(10), providing a natural right-handed neutrino candidate and unifying quarks and leptons. In the scheme of Ref. [10, 11], trilepton modes such as $p \rightarrow e^+ \nu \nu$ and $p \rightarrow \mu^+ \nu \nu$ could become significant. This work describes searches for these modes. Their observation, coupled with non-observation of $p \rightarrow e^+ \pi^0$, may allow for differentiation between PS and its SO(10) embedding [11]. Violating baryon and lepton number by two units ($|\Delta(B - L)| = 2$), unusual for standard decay channels, may lead to favorable implications for baryogenesis [12]. Interestingly, these trilepton proton decay modes were offered as an explanation [13, 14] of the atmospheric neutrino flavor “anomaly” [15, 16] before neutrino oscillations were established [17].

In this analysis, the data collected at Super-Kamiokande (SK) during the data taking periods of SK-I (May 1996-Jul 2001, 1489.2 live days), SK-II (Jan 2003-Oct 2005, 798.6 live days), SK-III (Sept 2006-Aug 2008, 518.1 live days) and the ongoing SK-IV experiment (Sept 2008-Oct 2013, 1632.3 live days), corresponding to a combined exposure of 273.4 kton · years, is analyzed. The 50 kiloton SK water Cherenkov detector (22.5 kton fiducial volume) is located beneath a one-km rock overburden (2700m water equivalent) in the Kamioka mine in Japan. Details of the detector design and performance in each SK period, as well as calibration, data reduction and simulation information can be found elsewhere [18, 19].

This analysis considers only events in which all observed Cherenkov light was fully contained within the inner detector.

The trilepton decay modes $p \rightarrow e^+ \nu \nu$ and $p \rightarrow \mu^+ \nu \nu$ are the first three-body nucleon decay searches undertaken by SK. Since the neutrinos cannot be observed, the only signature is the appearance of a charged lepton, e^+ or μ^+ . Accordingly, the invariant mass of the decay nucleon cannot be reconstructed. Unlike two-body decays, where each final-state particle carries away about half of the nucleon rest mass energy, in these three-body decays the charged lepton has a broad energy distribution, whose mean is 313 MeV for the decay of a free proton. Thus, atmospheric neutrino interactions dominate the lepton energy spectra and require a search for the proton decay signal superimposed on a substantial background. Limits on these modes from the IMB-3 [3] and Fréjus [20] experiments, 1.7×10^{31} and 2.1×10^{31} years, were obtained via simple counting techniques. In contrast, we employ energy spectrum fits. This technique is particularly well suited to three-body searches with large backgrounds as it takes full advantage of the signal and background spectral information.

The detection efficiency for nucleon decays in water is estimated from Monte Carlo (MC) simulations in which all protons within the H₂O molecule are assumed to decay with equal probability. Signal events are obtained by generating final state particles from the proton’s decay with energy and momentum uniformly distributed within the phase space. Conservation of kinematic variables constrain the processes to produce viable particle spectra. Specifics of the decay dynamics, which are model dependent but are not taken into account here, can play a role in determining the energy distributions of the resulting particles in three body decays. The assumption of a flat phase space, as employed within this analysis, was validated by comparing the final state charged lepton spectrum generated with a flat phase space to the spectrum originating from the three-body phase space of muon decay (reaction), as recently proposed [21] to account for decays encompassing a broad range of models. We have confirmed that adopting a non-flat phase space does not significantly alter the results of the analysis, because the charged lepton spectra do not have sufficiently different shapes (even for the decay of a free proton, which is minimally smeared). Thus, we conclude, that employing flat phase space in the signal simulation, which has been previously assumed in other similar searches [3, 20] without

much justification, is warranted.

In the signal simulation, the effects of Fermi momentum and the nuclear binding energy as well as nucleon-nucleon correlated decays are taken into account [22, 23]. Fermi momentum distributions are simulated using a spectral function fit to ^{12}C electron scattering data [24]. Considering only events generated within the fiducial volume (FV) of the detector, the signal MC consists of roughly 4000 events for each of the SK data periods.

Atmospheric neutrino background interactions are generated using the flux of Honda *et al.* [25] and the NEUT simulation package [26], which uses a relativistic Fermi gas model. The SK detector simulation [19] is based on the GEANT-3 [27] package. Background MC corresponding to a 500 year exposure of the detector is generated for each SK period.

The following event selection criteria are applied to the fully-contained data: (A) a single Cherenkov ring is present, (B) the ring is showering (electron-like) for $p \rightarrow e^+\nu\nu$ and non-showering (muon-like) for $p \rightarrow \mu^+\nu\nu$, (C) there are zero decay electrons for $p \rightarrow e^+\nu\nu$ and one decay electron for $p \rightarrow \mu^+\nu\nu$, (D) the reconstructed momentum lies in the range $100 \text{ MeV}/c \leq p_e \leq 1000 \text{ MeV}/c$ for $p \rightarrow e^+\nu\nu$ and in the range $200 \text{ MeV}/c \leq p_\mu \leq 1000 \text{ MeV}/c$ for $p \rightarrow \mu^+\nu\nu$. Reconstruction details may be found in Ref. [28]. The signal detection efficiency is defined as the fraction of events passing these selection criteria compared to the total number of events generated within the true fiducial volume (see Table I). The increase in efficiency seen in SK-IV for the $p \rightarrow \mu^+\nu\nu$ mode is caused by a 20% improvement in the detection of muon decay electrons after an upgrade of the detector electronics for this period [19].

In the case of $p \rightarrow e^+\nu\nu$, the dominant (78%) background after selection criteria are applied is due to ν_e quasi-elastic charged current (CCQE) interactions. The majority of the remaining background is due to ν_e and ν_μ charged current pion production (CC) as well as the all flavor's neutral current (NC) single pion production (12% and 5%, respectively). There are minor contributions from other processes such as coherent pion production (order of 1%). Similarly for the $p \rightarrow \mu^+\nu\nu$ mode, ν_μ CCQE interactions dominate (80%), with the largest remaining contribution coming from CC single pion production (15%). Additionally there are slight contributions from NC pion production, CC coherent and multiple-pion production (around 1% each). Processes not mentioned here are negligible.

A spectrum fit is performed on the reconstructed charged lepton momentum distributions of selected candidates. The foundation of the fit is a χ^2 minimization with systematic errors accounted for by quadratic penalties (“pull terms”) as described in Ref. [29]. The χ^2 function is defined as

$$\chi^2 = 2 \sum_{i=1}^{\text{nbins}} \left(z_i - N_i^{\text{obs}} + N_i^{\text{obs}} \ln \frac{N_i^{\text{obs}}}{z_i} \right) + \sum_{j=1}^{N_{\text{syserr}}} \left(\frac{\epsilon_j}{\sigma_j} \right)^2$$

$$z_i = \alpha \cdot N_i^{\text{back}} \left(1 + \sum_{j=1}^{N_{\text{syserr}}} f_i^j \frac{\epsilon_j}{\sigma_j} \right) + \beta \cdot N_i^{\text{sig}} \left(1 + \sum_{j=1}^{N_{\text{syserr}}} f_i^j \frac{\epsilon_j}{\sigma_j} \right), \quad (1)$$

where i labels the analysis bins. The terms N_i^{obs} , N_i^{sig} , N_i^{back} are the number of observed data, signal MC and background MC events in bin i . The MC expectation in a bin is taken to be $N_i^{\text{exp}} = \alpha \cdot N_i^{\text{back}} + \beta \cdot N_i^{\text{sig}}$, with α and β denoting the background (atmospheric neutrino) and signal (nucleon decay) normalizations. The j^{th} systematic error is accounted for by the “pull term”, where ϵ_j is the fit error parameter and f_i^j is the fractional change in the MC expectation bin due to a 1 sigma uncertainty σ_j of the error. A two-parameter fit is performed to the parameters α and β , with the point $(\alpha, \beta) = (1, 0)$ set to correspond to no signal hypothesis. With signal spectrum normalized by area to the background prior to the fit, $\beta = 1$ corresponds to the amount of nucleon decay events equal to the quantity of background MC after detector livetime normalization. The parameter space of (α, β) is allowed to vary in the intervals of $(\alpha \in [0.8, 1.2], \beta \in [0.0, 0.2])$. The χ^2 of Eq. (1) is minimized with respect to ϵ_j according to $\partial\chi^2/\partial\epsilon_j = 0$, yielding a set of equations which are solved iteratively, and the global minimum is defined as the best fit. The confidence level intervals are later derived from the χ^2 minimization at each point in the (α, β) plane after subtracting off this global minimum. Namely, the CL limit is based on the constant $\Delta\chi^2$ critical value corresponding to the 90% CL for a fit with one degree of freedom, after profiling out β 's dependence on α from the two-parameter fit.

Combining signal and background into each analysis MC expectation bin, as employed in a typical fit of this sort (see Ref. [29]), is an approximate approach where systematic errors for signal as well as background are applied to every analysis bin which contains both. In this analysis we employ a more accurate error treatment, splitting signal and background (doubling the number of analysis bins) for the application of systematic errors and then recombining them during the χ^2 minimization. A total of 72 momentum bins (18, 50-MeV/ c wide bins for each SK period) are considered for $p \rightarrow e^+\nu\nu$, corresponding to 144 MC bins when the background and signal are separated. In the case of $p \rightarrow \mu^+\nu\nu$ a total of 64 momentum bins (16, 50-MeV/ c wide bins for each SK period) are used in the analysis, corresponding to 128 MC bins with background and signal separated.

Systematic errors may be divided into several categories: background systematics, detector and reconstruction systematics, and signal systematics. Detector and

TABLE I: Best fit parameter values, signal detection efficiency for each SK running period, 90% C.L. value of β parameter, allowed number of nucleon decay events in the full 273.4 kiloton \cdot year exposure (SK-I: 91.7, SK-II: 49.2, SK-III: 31.9, SK-IV: 100.5) and a partial lifetime limit for each decay mode at 90% C.L.

Decay mode	Best fit values (α, β)	Signal efficiency for SK-I, -II, -III, -IV (%) (efficiency uncertainty)	$\beta_{90\text{CL}}$	Signal events at 90% C.L. ($N_{90\text{CL}}$)	τ/\mathcal{B} ($\times 10^{32}$ yrs)
$p \rightarrow e^+ \nu \nu$	(1.05, 0.03)	88.8, 88.0, 89.2, 87.8 ($\pm 0.5, \pm 0.5, \pm 0.5, \pm 0.5$)	0.06	459	1.7
$p \rightarrow \mu^+ \nu \nu$	(0.99, 0.02)	64.4, 65.0, 67.0, 78.4 ($\pm 0.7, \pm 0.7, \pm 0.7, \pm 0.6$)	0.05	286	2.2

TABLE II: Systematic errors of the nucleon decay spectrum fits, with 1σ uncertainties and resulting fit pull terms. Errors specific to signal and background are denoted by S and B, while those that are common to both by SB.

Decay mode		$p \rightarrow e^+ \nu \nu$	$p \rightarrow \mu^+ \nu \nu$	
Systematic error	1- σ uncertainty (%)	Fit pull (σ)	Fit pull (σ)	
Final state interactions (FSI)	10	0.08	-0.55	B
Flux normalization ($E_\nu < 1$ GeV)	25 ^a	-0.36	-0.42	B
Flux normalization ($E_\nu > 1$ GeV)	15 ^b	-0.86	-0.90	B
M_A in ν interactions	10	0.32	0.48	B
Single meson cross-section in ν interactions	10	-0.36	-0.16	B
Energy calibration of SK-I, -II, -III, -IV	1.1, 1.7, 2.7, 2.3	0.51, -1.01, 0.44, 0.39	-0.50, 0.06, -0.16, 0.25	SB
Fermi model comparison	10 ^c	-0.25	0.02	S
Nucleon-nucleon correlated decay	100	-0.05	0.01	S

^aUncertainty linearly decreases with $\log E_\nu$ from 25% (0.1 GeV) to 7% (1 GeV).

^bUncertainty is 7% up to 10 GeV, linearly increases with $\log E_\nu$ from 7% (10 GeV) to 12% (100 GeV) and then 20% (1 TeV).

^cComparison of spectral function and Fermi gas model.

reconstruction systematics are common to both signal and background.

This study starts by considering all 154 systematic uncertainties which are taken into account in the standard SK neutrino oscillation analysis [30], along with two signal-specific systematic effects related to correlated decays and Fermi momentum. In order to select which systematic uncertainties to include in the limit calculation, only error terms with at least one $|f_i^j| > 0.05$ are used in the analysis. Loosening the selection to $|f_i^j| > 0.01$ does not significantly affect the analyses results but greatly increases the number of errors to be treated. After selection, there are 11 systematic error terms for both $p \rightarrow e^+ \nu \nu$ and $p \rightarrow \mu^+ \nu \nu$. The main systematic contributions originate from energy calibration uncertainties (common error to both signal and background), uncertainties related to the atmospheric neutrino flux, and uncertainties in the signal simulation. The complete list of errors, their uncertainties, and fitted pull terms can be found in Table II. Errors specific to signal and background are denoted by S and B, respectively, while those

that are common to both are denoted by SB.

Performing the fit allows us to obtain the overall background and signal normalizations α and β . For the mode $p \rightarrow e^+ \nu \nu$ the data's best fit point is found to be $(\alpha, \beta) = (1.05, 0.03)$ with $\chi^2 = 65.6/70$ dof, while for $p \rightarrow \mu^+ \nu \nu$ the result is $(\alpha, \beta) = (0.99, 0.02)$ with $\chi^2 = 66.1/62$ dof. The $\Delta\chi^2 (= \chi^2 - \chi_{\min}^2)$ values corresponding to no proton decay signal being present, are 1.5 and 0.5 for $p \rightarrow e^+ \nu \nu$ and $p \rightarrow \mu^+ \nu \nu$ modes respectively. These outcomes are consistent with no signal present at 1σ level. Extracting the 90% confidence level allowed value of β ($\beta_{90\text{CL}}$) from the fit, which is found to be 0.06 for $p \rightarrow e^+ \nu \nu$ and 0.05 for $p \rightarrow \mu^+ \nu \nu$ respectively, a lower lifetime limit on these decays can be set. From $\beta_{90\text{CL}}$ the amount of signal allowed at the 90% confidence level can be computed as $N_{90\text{CL}} = \beta_{90\text{CL}} \cdot N^{\text{signal}}$. The partial lifetime limit for each decay mode is then calculated according to

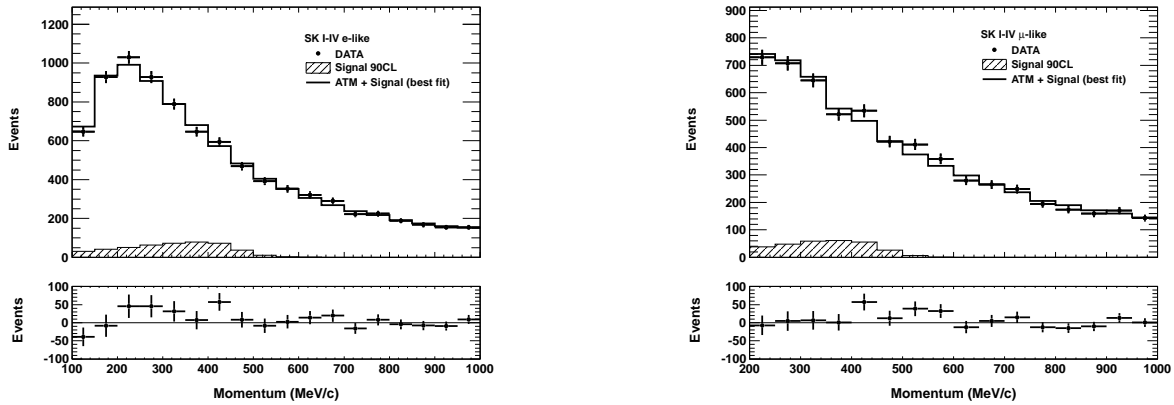


FIG. 1: Reconstructed momentum distribution for 273.4 kton · years of combined SK data (black dots), the best fit result for the atmospheric neutrino background and signal Monte Carlo (solid line) as well as the 90% confidence level allowed amount of nucleon decay (hatched histogram) for $p \rightarrow e^+\nu\nu$ (left) and $p \rightarrow \mu^+\nu\nu$ (right). Residuals from data after background subtraction (bottom histograms).

$$\tau_{90\text{CL}}/\mathcal{B} = \frac{\sum_{\text{sk=SK1}}^{\text{SK4}} \lambda_{\text{sk}} \cdot \epsilon_{\text{sk}} \cdot N^{\text{nucleons}}}{N_{90\text{CL}}}, \quad (2)$$

where \mathcal{B} represents the branching ratio of a process, N^{nucleons} is the number of nucleons per kiloton of water (3.3×10^{32} protons), ϵ_{sk} is the signal efficiency in each SK phase, λ_{sk} is the corresponding exposure in kiloton · years, and $N_{90\text{CL}}$ is the amount of signal allowed at the 90% confidence level. The signal efficiency, number of decay sources, as well as the signal normalization values used for the lifetime calculation can be found in Table I. The fitted momentum spectra as well as residuals for both modes appear in Figure 1. Momentum spectra for the 273.4 kton · years of combined SK data (black dots), the best-fit result for the atmospheric neutrino background and signal Monte Carlo (solid line) as well as the amount of nucleon decay allowed at the 90% confidence level (hatched histogram) for $p \rightarrow e^+\nu\nu$ (left) and $p \rightarrow \mu^+\nu\nu$ (right) are shown. Residuals from data after background MC is subtracted are also depicted (bottom histograms). From the analysis we set partial lifetime limits of 1.7×10^{32} and 2.2×10^{32} years for $p \rightarrow e^+\nu\nu$ and $p \rightarrow \mu^+\nu\nu$, respectively. The sensitivity to these modes is calculated to be 2.7×10^{32} and 2.5×10^{32} years. The lifetime limits found in this study are an order of magnitude improvement over the previous results [3, 20]. These results provide strong constraints to both the permitted parameter space of Refs. [11, 12], which predict lifetimes of around $10^{30} - 10^{33}$ years, and on other GUT models which allow for similar processes. We note, that the analyses presented in this work are only weakly model dependent, due to the assumption of a flat phase space in the signal generation. However, this assumption agrees well with alternative phase space considerations [21] in

the context of vector- or scalar-mediated proton decays, which are typical of GUT models [1, 2, 9].

We gratefully acknowledge cooperation of the Kamioka Mining and Smelting Company. The Super-Kamiokande experiment was built and has been operated with funding from the Japanese Ministry of Education, Culture, Sports, Science and Technology, the United States Department of Energy, and the U.S. National Science Foundation. Some of us have been supported by funds from the Korean Research Foundation (BK21), the National Research Foundation of Korea (NRF-20110024009), the State Committee for Scientific Research in Poland (grant1757/B/H03/2008/35), the Japan Society for Promotion of Science, and the National Natural Science Foundation of China under Grants No.10575056.

* Deceased.

- [1] H. Georgi and S. Glashow, Phys.Rev.Lett. **32**, 438 (1974).
- [2] H. Fritzsch and P. Minkowski, Annals Phys. **93**, 193 (1975).
- [3] C. McGrew, R. Becker-Szendy, C. Bratton, J. Breault, D. Cady, et al. (IMB-3 Collaboration), Phys.Rev. **D59**, 052004 (1999).
- [4] K. Hirata et al. (KAMIOKANDE-II Collaboration), Phys.Lett. **B220**, 308 (1989).
- [5] M. Shiozawa et al. (Super-Kamiokande Collaboration), Phys.Rev.Lett. **81**, 3319 (1998), hep-ex/9806014.
- [6] K. Kobayashi et al. (Super-Kamiokande Collaboration), Phys.Rev. **D72**, 052007 (2005), hep-ex/0502026.
- [7] S. Chatrchyan et al. (CMS Collaboration), Phys.Rev. **D88**, 052017 (2013), 1301.2175.
- [8] G. Aad et al. (ATLAS Collaboration), Phys.Rev.Lett. **106**, 131802 (2011), 1102.2357.

- [9] J. C. Pati and A. Salam, Phys.Rev. **D10**, 275 (1974).
- [10] J. C. Pati, A. Salam, and U. Sarkar, Phys.Lett. **B133**, 330 (1983).
- [11] J. C. Pati, Phys.Rev. **D29**, 1549 (1984).
- [12] P.-H. Gu and U. Sarkar (2011), 1110.4581.
- [13] W. Mann, T. Kafka, and W. Leeson, Phys.Lett. **B291**, 200 (1992).
- [14] P. J. O'Donnell and U. Sarkar, Phys.Lett. **B316**, 121 (1993), hep-ph/9307254.
- [15] R. Becker-Szendy, C. Bratton, D. Casper, S. Dye, W. Gajewski, et al. (IMB-3 Collaboration), Phys.Rev. **D46**, 3720 (1992).
- [16] Y. Fukuda et al. (Kamiokande Collaboration), Phys.Lett. **B335**, 237 (1994).
- [17] Y. Fukuda et al. (Super-Kamiokande Collaboration), Phys.Rev.Lett. **81**, 1562 (1998), hep-ex/9807003.
- [18] Y. Fukuda et al. (Super-Kamiokande Collaboration), Nucl.Instrum.Meth. **A501**, 418 (2003).
- [19] K. Abe, Y. Hayato, T. Iida, K. Iyogi, J. Kameda, et al., Nucl.Instrum.Meth. **A737**, 253 (2014), 1307.0162.
- [20] C. Berger et al. (Frejus Collaboration), Phys.Lett. **B269**, 227 (1991).
- [21] M.-C. Chen and V. Takhistov, Phys.Rev. **D89**, 095003 (2014), 1402.7360.
- [22] H. Nishino et al. (Super-Kamiokande), Phys.Rev. **D85**, 112001 (2012), 1203.4030.
- [23] C. Regis et al. (Super-Kamiokande Collaboration), Phys.Rev. **D86**, 012006 (2012), 1205.6538.
- [24] K. Nakamura, S. Hiramatsu, T. Kamae, H. Muramatsu, N. Izutsu, et al., Nucl.Phys. **A268**, 381 (1976).
- [25] M. Honda, T. Kajita, K. Kasahara, S. Midorikawa, and T. Sanuki, Phys.Rev. **D75**, 043006 (2007), astro-ph/0611418.
- [26] Y. Hayato, Nucl.Phys.Proc.Suppl. **112**, 171 (2002).
- [27] R. Brun, F. Carminati, and S. Giani (1994).
- [28] M. Shiozawa (Super-Kamiokande Collaboration), Nucl.Instrum.Meth. **A433**, 240 (1999).
- [29] G. Fogli, E. Lisi, A. Marrone, D. Montanino, and A. Palazzo, Phys.Rev. **D66**, 053010 (2002), hep-ph/0206162.
- [30] R. Wendell et al. (Super-Kamiokande Collaboration), Phys.Rev. **D81**, 092004 (2010), 1002.3471.